Journal of Physics: Conference Series **1342** (2020) 012005 doi:10.1088/1742-6596/1342/1/012005

Searching for neutrinoless double beta decay with GERDA

M. Agostini[o], A.M. Bakalyarov[m], M. Balata[a], I. Barabanov[k], L. Baudis[s], C. Bauer[g], E. Bellotti[h,i], S. Belogurov[l,k], A. Bettini[p,q], L. Bezrukov[k], T. Bode[o], V. Brudanin[e], R. Brugnera[p,q], A. Caldwell[n], C. Cattadori[i], A. Chernogorov[l], V. D'Andrea[a], E.V. Demidova[l], N. Di Marco[a], A. Domula[d], E. Doroshkevich[k], V. Egorov[e], R. Falkenstein[r], A. Gangapshev[k,g], A. Garfagnini[p,q], C. Gooch[n], P. Grabmayr[r], V. Gurentsov[k], K. Gusev[e,m,o], J. Hakenmüller[g], A. Hegai[r], M. Heisel[g], S. Hemmer[q], R. Hiller[s], W. Hofmann[g], M. Hult[f], L.V. Inzhechik[k], J. Janicskó Csáthy[o], J. Jochum[r], M. Junker[a], V. Kazalov[k], Y. Kermaidic[g], T. Kihm[g], I.V. Kirpichnikov[l], A. Kirsch[g], A. Kish[s], A. Klimenko[g,e], R. Kneißl[n], K.T. Knöpfle[g], O. Kochetov[e], V.N. Kornoukhov[l,k], V.V. Kuzminov[k], M. Laubenstein[a], A. Lazzaro[o], V.I. Lebedev[m], M. Lindner[g], I. Lippi[q], A. Lubashevskiy[g,e], B. Lubsandorzhiev[k], G. Lutter[f], C. Macolino[a], B. Majorovits[n], W. Maneschg[g], M. Miloradovic[s], R. Mingazheva[s], M. Misiaszek[c], P. Moseev[k], I. Nemchenok[e], K. Panas[c], L. Pandola[b1], K. Pelczar[a], A. Pullia[j], C. Ransom[s], S. Riboldi[j], N. Rumyantseva[m,e], C. Sada[p,q], F. Salamida[i], C. Schmitt[r], B. Schneider[d], J. Schreiner[g], O. Schulz[n], B. Schwingenheuer[g], S. Schönert[o], A-K. Schütz[r], O. Selivanenko[k], E. Shevchik[e], M. Shirchenko[e], H. Simgen[g], A. Smolnikov[g,e], L. Stanco[q], L. Vanhoefer[n], A.A. Vasenko[l], A. Veresnikova[k], K. von Sturm[p,q], V. Wagner[g], A. Wegmann[g], T. Wester[d], C. Wiesinger[o], M. Wojcik[c], E. Yanovich[k], I. Zhitnikov[e], S.V. Zhukov[m], D. Zinatulina[e], A.J. Zsigmond[n], K. Zuber[d], G. Zuzel[c]

[a] INFN Laboratori Nazionali del Gran Sasso and Gran Sasso Science Institute, Assergi, Italy
[b] INFN Laboratori Nazionali del Sud, Catania, Italy
[c] Institute of Physics, Jagiellonian University, Cracow, Poland
[d] Institut für Kern- und Teilchenphysik, Technische Universität Dresden, Dresden, Germany
[e] Joint Institute for Nuclear Research, Dubna, Russia
[f] European Commission, JRC-Geel, Geel, Belgium
[g] Max-Planck-Institut für Kernphysik, Heidelberg, Germany
[h] Dipartimento di Fisica, Università Milano Bicocca, Milan, Italy
[i] INFN Milano Bicocca, Milan, Italy
[j] Dipartimento di Fisica, Università degli Studi di Milano e INFN Milano, Milan, Italy
[k] Institute for Nuclear Research of the Russian Academy of Sciences, Moscow, Russia
[l] Institute for Theoretical and Experimental Physics, Moscow, Russia
[m] National Research Centre "Kurchatov Institute", Moscow, Russia
[n] Max-Planck-Institut für Physik, Munich, Germany

[1] Speaker

[o] Physik Department and Excellence Cluster Universe, Technische Universität München, Germany
[p] Dipartimento di Fisica e Astronomia dell'Università di Padova, Padua, Italy
[q] INFN Padova, Padua, Italy
[r] Physikalisches Institut, Eberhard Karls Universität Tübingen, Tübingen, Germany
[s] Physik Institut der Universität Zürich, Zurich, Switzerland

E-mail: pandola@lns.infn.it

Abstract. The GERmanium Detector Array (GERDA) experiment located at the INFN Gran Sasso Laboratory (Italy), is looking for the neutrinoless double beta decay of ^{76}Ge, by using high-purity germanium detectors made from isotopically enriched material. The combination of the novel experimental design, the careful material selection for radio-purity and the active/passive shielding techniques result in a very low residual background at the Q-value of the decay, about 10^{-3} cts/(keV·kg·yr). This makes GERDA the first experiment in the field to be background-free for the complete design exposure of 100 kg·yr. A search for neutrinoless double beta decay was performed with a total exposure of 46.7 kg·yr: 23.2 kg·yr come from the second phase (Phase II) of the experiment, in which the background is reduced by about a factor of ten with respect to the previous phase. The analysis presented in this paper includes 12.4 kg·yr of new Phase II data. No evidence for a possible signal is found: the lower limit for the half-life of ^{76}Ge is $8.0 \cdot 10^{25}$ yr at 90% CL. The experimental median sensitivity is $5.8 \cdot 10^{25}$ yr. The experiment is currently taking data. As it is running in a background-free regime, its sensitivity grows linearly with exposure and it is expected to surpass 10^{26} yr within 2018.

1. Introduction

Neutrinoless double beta ($0\nu\beta\beta$) decay is a hypothetical nuclear transition in which a nucleus (A, Z) decays as $(A, Z) \rightarrow (A, Z + 2) + 2e^-$. Neutrinoless double beta decay is forbidden by the Standard Model (SM), as it violates by two units the conservation of the lepton number. A SM-allowed version of double beta decay also exists ($2\nu\beta\beta$), in which the final state includes two anti-neutrinos. This rare SM process has been observed experimentally in about ten nuclei, with half-lives in the range of $10^{18} - 10^{24}$ yr.

$0\nu\beta\beta$ decay is a far more interesting research topic than $2\nu\beta\beta$, as it is a unique probe to physics beyond the SM. The observation of $0\nu\beta\beta$ decay would prove in fact that neutrinos have a Majorana mass component [1, 2] and that lepton number is not conserved, thus shedding a new light on fundamental issues as the matter-antimatter asymmetry and the origin of neutrino masses [3, 4, 5]. For this reason a wide experimental effort is placed worldwide in the search for neutrinoless double beta decay of several candidate nuclei, most notably ^{76}Ge [6, 7], ^{136}Xe [8, 9, 10] and ^{130}Te [11, 12]. The current best limits on the $0\nu\beta\beta$ half-life lie in the range of $10^{24} - 10^{26}$ yr, depending on the specific nucleus. It is clear that any experimental attempt to detect such long half-lives – corresponding to decay rates smaller than 1 decay/(kg·yr) – requires a very strong suppression of all background sources. This calls for the use of innovative low-background techniques (shielding, active vetoes, material selection for low-radioactivity) in a suitably-deep underground laboratory.

2. The GERDA experiment

The GERmanium Detector Array (GERDA) experiment [13] at the underground Laboratori Nazionali del Gran Sasso (LNGS) of INFN searches for the $0\nu\beta\beta$ decay of ^{76}Ge, using high-purity germanium (HPGe) detectors isotopically enriched to about 87% in ^{76}Ge. The experiment is located in the Hall A of LNGS, under a rock overburden of 3500 m w.e.

The two electrons emitted in $0\nu\beta\beta$ decay have a range of $\sim$ 1 mm in germanium, so that in most cases their kinetic energy is entirely deposited within the detector itself. The

experimental signature is hence a mono-energetic energy release at the Q-value of the decay, which is $Q_{\beta\beta} = 2039$ keV for ^{76}Ge. A key feature of HPGe detectors is the excellent energy resolution, better than 4 keV full width at half maximum (FWHM) at $Q_{\beta\beta}$. The very good energy resolution allows for a narrow search region for the $0\nu\beta\beta$ signal, thus minimizing the background, and for the convincing identification of a narrow line at the expected energy, in case of a discovery.

The key design feature of GERDA is the operation of bare HPGe detectors directly immersed in liquid argon (LAr). Liquid argon, contained in a 64 m^3 cryostat, acts as cooling medium and as a shielding against the external radiation. The cryostat is enclosed in a stainless steel water tank containing 590 m^3 of ultra-pure water, serving as additional shielding and effective neutron moderator. The water tank is equipped with photomultipliers, such that the water volume is operated as a Cerenkov detector to veto the residual cosmic ray muons in the underground laboratory. The HPGe detectors are arranged as a closely-packed array of seven strings, that are deployed in the LAr cryostat through a neck on the top, as shown in Fig. 1. Two sets of detectors enriched in ^{76}Ge ($^{\text{enr}}$Ge) are currently operated in GERDA: refurbished p-type coaxial detectors, that were previously operated by the Heidelberg-Moscow [14] and IGEX [15] experiments; and new Broad Energy Germanium (BEGe) p-type detectors, manufactured by Canberra. The BEGe detectors are designed to provide much superior pulse shape discrimination performance with respect to the old-style coaxial detectors [16, 17]. The charge signals from the HPGe detectors are sampled for a total window of 160 μs and stored on disk. Data are analyzed offline using the GELATIO software package [18] and the procedures described in [19, 20].

As LAr is a very effective scintillator, the LAr volume surrounding the detector array is equipped with photo-detectors and operated as an active veto. In particular, the HPGe strings are enclosed by a curtain of scintillating fibers coated with a wavelength shifter, in order to convert the wavelength from the original 128 nm of the argon scintillation to the visible range. The light collected by the fibers is detected by 90 SiPM, arranged in 15 read-out channels. The LAr light detection system is complemented by a set of 16 low-radioactivity photomultipliers, placed above and below the HPGe strings.

The experiment had been designed to proceed through two phases. The first phase (Phase I), from November 2011 to May 2013, accumulated an exposure of 21.6 kg·yr with a background of about 10^{-2} cts/(keV·kg·yr) at $Q_{\beta\beta}$ [19]. The LAr volume was not instrumented with photosensors and it was hence used as a pure passive shield. The second phase (Phase II) is ongoing since December 2015: it features the full instrumentation of the LAr volume and the doubling of the mass of $^{\text{enr}}$Ge detectors, by the deployment of new BEGe detectors. In total, 37 $^{\text{enr}}$Ge detectors are available in Phase II, 30 BEGe (20.0 kg) and 7 coaxial (15.6 kg). The goal of Phase II is to accumulate 100 kg·yr of exposure with a background of 10^{-3} cts/(keV·kg·yr), i.e. an order of magnitude smaller with respect to Phase I. As in Phase I, the data taking follows a blind analysis strategy: all events in the Ge detectors with reconstructed energy within $Q_{\beta\beta}\pm25$ keV, i.e. close to the expected signal region, are stored on disk but not made available for analysis. The blinding is released approximately every year, after all analysis cuts are tested and finalized.

The initial Phase II results were released in June 2016 with 10.8 kg·yr total exposure, indicating that the ambitious background goal has indeed been met [6]. The expected background in the signal search region $Q_{\beta\beta}\pm0.5$ FWHM is $\lesssim 1$ count for the full design exposure, thus making GERDA to be the first "background-free" experiment in the field. The sensitivity is expected to grow linearly with the exposure $\mathcal{E}$ for the entire data taking period, instead of the $\sqrt{\mathcal{E}}$ regime of background-dominated experiments.

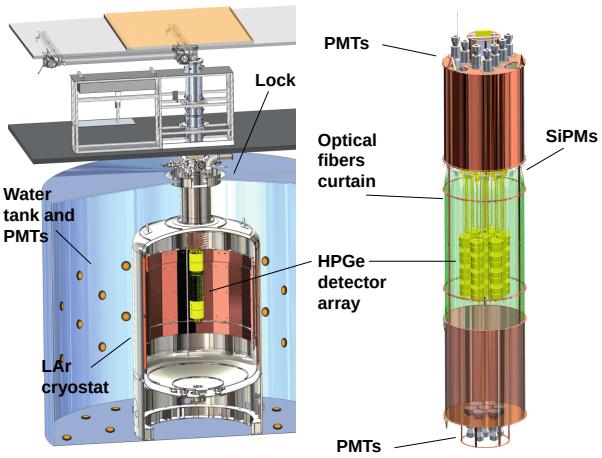

Figure 1. Schematic layout of the GERDA setup. The right-hand side of the figure displays a zoom of the inner part of the setup.

3. Data taking and selection

The Phase II data taking is ongoing since December 25^{th}, 2015. Data collected up to April 15^{th}, 2017 (477.2 calendar days) have been fully validated and analyzed, totaling an $^{\text{enr}}$Ge exposure of 34.4 kg·yr (18.2 kg·yr from BEGe detectors and 16.2 kg·yr from coaxial detectors). The exposure is hence increased by a factor of three with respect to the previous Phase II release [6].

The Ge event energy is reconstructed offline using the Zero Area Cusp (ZAC) algorithm [21], which is optimized for each detector and each calibration individually. The energy scale is set by taking weekly calibration runs with ^{228}Th sources. Given the excellent energy resolution of HPGe detectors, the energy scale at $Q_{\beta\beta}$ must be stable within $\lesssim 2$ keV throughout the data taking. The stability of the system is monitored weekly, by checking the shifts of the γ-lines between two consecutive calibrations, and continuously, by injecting charge pulses of fixed amplitude (test pulses) every 20 s. Periods in which the energy scale exhibits jumps or drifts exceeding 2 keV are discarded from the analysis. The remarkable stability of the 2615 keV γ-line from the ^{228}Th source between two consecutive calibrations is displayed in Fig. 2a. The energy resolution at $Q_{\beta\beta}$ is also evaluated by using the calibration data. Resolution vs. energy is parametrized as $\sigma(E) = \sqrt{a + bE}$; the free parameters a and b are evaluated, for coaxial and BEGe detectors separately, by a fit of the ^{228}Th γ-lines (see Fig. 2b). Nevertheless, it is observed for the coaxial detectors that the energy resolution achieved in the physics data for the ^{40}K and ^{42}K lines (1460 and 1525 keV, respectively) is slightly worse than the expectation based on calibrations. This could be due to long-period gain fluctuations and instabilities taking place during the multi-week physics runs. The effect is accounted for by including a further summation term in the formula above, such to match the observed resolution of the ^{40}K and ^{42}K peaks in the physics data. No correction is required for the BEGe detectors, as shown in Fig. 2b. The average resolution at $Q_{\beta\beta}$ is 3.90(7) keV and 2.93(6) keV FWHM for the $^{\text{enr}}$Ge coaxial and BEGe detectors, respectively.

Unphysical events, e.g. due to discharges, are effectively removed by means of a set of dedicated quality cuts based on features of the digitized traces, as baseline flatness, polarity and time structure. The loss of genuine $0\nu\beta\beta$ signals due to mis-classification by the quality cuts is estimated to be smaller than 0.1%, based on the acceptance of γ-lines in calibration data, test pulse events and simulated template signals. The peculiar topology of $0\nu\beta\beta$ decay and the signature which is used for the search (i.e. full energy deposition at $Q_{\beta\beta}$) allow to

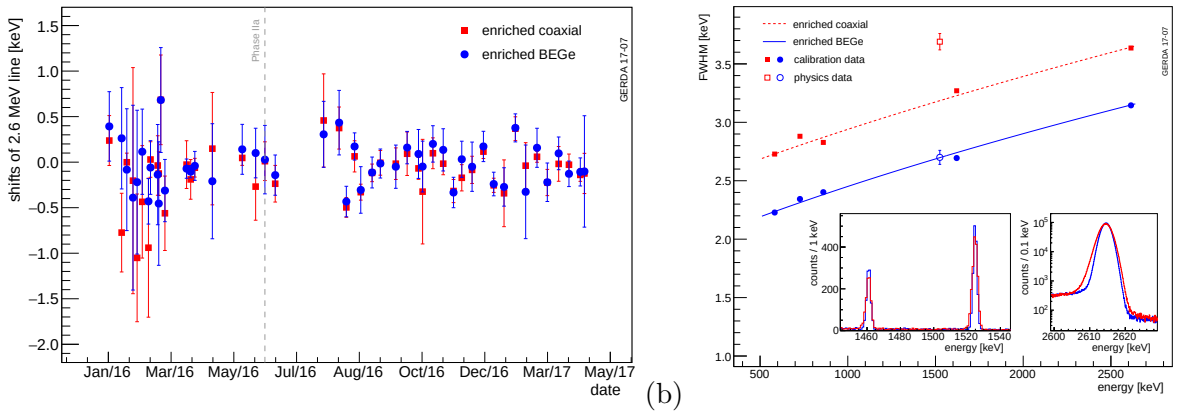

Figure 2. (a) Average shift of the 2615 keV γ-ray line from the ^{228}Th between consecutive calibrations. The error bars represent the standard deviation of the shifts of the individual detectors. (b) Average energy resolution for γ lines observed in calibration data and in physics data, for the BEGe and coaxial detectors. The inset displays a zoom of the γ lines at 1460 keV (^{40}K) and 1525 keV (^{42}K) in physics data, and a zoom of the 2615 keV line from calibration data.

define efficient analysis cuts, featuring high selection efficiency and high ability to reject the α and γ background. The target events of GERDA are those in which the whole energy $Q_{\beta\beta}$ is released within one HPGe detector, which happens for about 83% of decays taking place in the detector itself. The probability above accounts for the presence of an inactive volume inside the detectors and for the possibility that energy partially escapes, e.g. via bremsstrahlung or x-rays. Events in which more than one Ge detector has an energy deposit, or in which an energy deposit in liquid argon is detected within 5 μs from the Ge signal, are rejected as background events. The LAr-veto inefficiency is (2.3 ± 0.1)%, due to random coincidences which falsely produce the rejection of a $0\nu\beta\beta$ decay. Furthermore, Ge events in coincidence with a muon veto signal within a 10 μs window are also discarded.

Genuine $0\nu\beta\beta$ decays produce a very localized energy deposit, due to the short range of electrons in Ge, and are predominantly single-site events (SSEs). The most important background sources are either γ-rays, which mostly interact by multiple Compton scattering separated by $\sim$ 1 cm in Ge (multi-site event, MSE), or external α/β-rays, which deposit their energy on the detector surface. Given this difference, the time profile of the Ge current signal can be used to discriminate single-site events against multi-site or surface background events. The selection cuts are set for each detector individually; they are defined by using the double escape peak (DEP) of the 2615 keV line of the ^{228}Th calibrations as a proxy for signal events.

The electric field configuration of BEGe detectors allows for a very effective mono-parametric pulse shape discrimination (PSD), based on the ratio A/E between the maximum amplitude A of the current signal and the total energy E [16, 17, 22]. The A/E parameter is corrected to account for time and energy dependence and normalized as described in Ref. [23]. The cut on A/E allows to reject > 90% of (γ-like) MSEs and basically all α-like surface events. The $0\nu\beta\beta$ selection efficiency is (87 ± 2)%. Pulse shape discrimination is less effective for the coaxial detectors and cannot be performed with a single parameter [17]. Two artificial neural network (ANN) algorithms are instead used, to classify SSE vs. MSE and internal vs. α surface events, respectively. The first network is trained with calibration events from the DEP of ^{208}Tl at 1592 keV (SSE sample) and from the nearby γ-line at 1620 keV from ^{212}Bi (MSE sample), respectively. The second network is trained using $2\nu\beta\beta$ events (internal sample) and α events (surface sample) from physics data. The selection efficiency of the ANNs is evaluated by applying

Table 1. Summary of the Phase I and Phase II analysis data sets (exposure, energy resolution, total efficiency and background index). Background is evaluated in the range between 1930 and 2190 keV, excluding the intervals (2104 ± 5) keV and (2119 ± 5) keV, where known background peaks are expected, and the signal interval $(Q_{\beta\beta} \pm 5)$ keV.

Data set	Exposure (kg·yr)	Resolution at $Q_{\beta\beta}$ (keV) FWHM	Efficiency ϵ	Background Index 10^{-3} cts/(keV·kg·yr)
Phase I golden [19]	17.9	4.3(1)	0.57(3)	11 ± 2
Phase I silver [19]	1.3	4.3(1)	0.57(3)	30 ± 10
Phase I BEGe [19]	2.4	2.7(2)	0.66(2)	5^{+4}_{-3}
Phase I extra [6]	1.9	4.2(2)	0.58(4)	5^{+4}_{-3}
Total Phase I	23.5			
Phase II coaxial [6]	5.0	4.0(2)	0.53(5)	$3.5^{+2.1}_{-1.5}$
Phase II BEGe	18.2	2.93(6)	0.60(2)	$1.0^{+0.6}_{-0.4}$
Total Phase II	23.2			
Total Phase I and II	46.7			

the selection to a sample of $2\nu\beta\beta$ events and to traces simulated by a dedicated Monte Carlo code [24]. The combined selection efficiency for $0\nu\beta\beta$ decays is $(79 \pm 5)\%$.

4. Statistical analysis and results

Data from the BEGe detectors taken between June 1, 2016 and April 15, 2017 have been disclosed in June 2017, totaling 12.4 kg·yr of additional exposure with respect to Ref. [6]. Only two extra events are found which pass all selection cuts; both of them are more than 15 keV away from $Q_{\beta\beta}$ (namely $> 10\sigma$) and cannot hence be attributed to $0\nu\beta\beta$ decay. Data from the coaxial detectors (11.2 kg·yr) were not unblinded because it was recently realized that a fraction of α-induced events, that are characterized by a very short rise time are not correctly identified by the ANN PSD and leak as candidate $0\nu\beta\beta$ events. As these events are clearly background, data are to be unblinded only when the PSD is upgraded and the new cut is frozen.

The exposure available for analysis is 23.5 kg·yr and 23.2 kg·yr for Phase I and Phase II, respectively, totaling (236.9 ± 4.6) mol·yr of ^{76}Ge in the active volume of the detectors. Data are grouped into six data sets, according to the detector type (and energy resolution) and to the background at $Q_{\beta\beta}$, as listed in Table 1. The statistical analysis is described in the Methods Section of Ref. [6]: it is performed as a simultaneous unbinned maximum likelihood fit of the energy spectrum of the six data sets D_i in the range between 1930 and 2190 keV. The fit range excludes the intervals (2104 ± 5) keV and (2119 ± 5) keV, where known background peaks are expected, such that it spans $\Delta E = 240$ keV in total. For a given $0\nu\beta\beta$ signal strength $S{=}1/T^{0\nu}_{1/2}$ the expected number of identified signal events in a data set is given by: $\mu_i^S = \frac{\ln 2 \mathcal{N}_A}{m_a} \epsilon_i \mathcal{E}_i S$ where $\mathcal{N}_A$ is Avogadro's number, m_a the molar mass, ϵ_i the total efficiency and $\mathcal{E}_i$ the exposure (i.e. detector mass $\times$ time). The efficiency ϵ_i accounts globally for: the enrichment fraction of ^{76}Ge in $^{\text{enr}}$Ge; the probability that the entire decay energy $Q_{\beta\beta}$ is released in the active fraction of the Ge detector; the efficiency of the offline reconstruction and of all cuts. Similarly, the expected number of background events surviving the selection cuts is calculated as $\mu_i^B = \mathcal{E}_i B_i \Delta E$ where B_i is the background index. Each data set spectrum is fitted with a function made by a Gaussian distribution at $Q_{\beta\beta}$ for the signal and a flat distribution for the background. The common signal strength S and all backgrounds B_i are bound to positive values.

The same likelihood function is used to perform the analysis in a frequentist and in a Bayesian

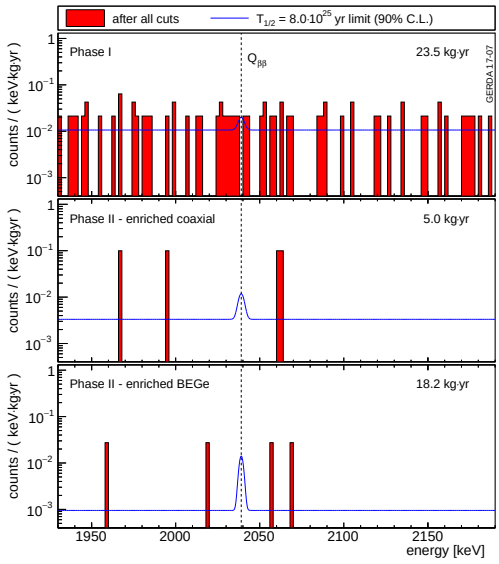

Figure 3. Energy spectra around $Q_{\beta\beta}$ for Phase I, Phase II coaxial detectors and Phase II BEGe detectors after all cuts. The binning is 2 keV. The blue lines show the hypothetical $0\nu\beta\beta$ signal for $T^{0\nu}_{1/2}= 8.0 \cdot 10^{25}$ yr, sitting on the constant background.

framework. The frequentist analysis employs a test statistics $t_S = -2 \ln \lambda(S)$ based on the profile likelihood $\lambda(S)$ [25]. Due to the low-statistics regime of GERDA, Wilks's theorem is not valid, typically yielding under-coverage. The confidence intervals are derived by using a toy Monte Carlo approach, which ensures the correct coverage by construction. For each assumption of the signal strength S the full distribution $f(t_S)$ of the test statistics is built and the p-value for the observed data is calculated. The analysis of the GERDA data returns a best-fit $S = 0$ (i.e. no signal). The limit on the half-life of ^{76}Ge is $T^{0\nu}_{1/2} > 8.0 \cdot 10^{25}$ yr (90% CL). The median sensitivity for the 90% CL lower limit of $T^{0\nu}_{1/2}$ is $5.8 \cdot 10^{25}$ yr. It is calculated by producing Monte Carlo realizations of GERDA with different signal strengths and evaluating the test-statistics for the null hypothesis. The probability to produce a limit stronger than the actual one within an ensemble of Monte Carlo GERDA realizations is about 30%.

A statistical analysis within the Bayesian framework is also available. The posterior probability of the signal strength $P(S)$ is calculated according to Bayes's theorem, after marginalization of all other nuisance parameters. A flat prior between 0 and 10^{-24} 1/yr is taken for the signal strength. The 90% credible interval obtained from the analysis is $T^{0\nu}_{1/2} > 5.1 \cdot 10^{25}$ yr; it is calculated as the minimum interval of the posterior probability $P(S)$ which contains 90% of the probability. The median sensitivity is $T^{0\nu}_{1/2} > 4.5 \cdot 10^{25}$ yr; as for the frequentist analysis, it is evaluated by repeating the full analysis procedure for a large set of Monte Carlo realizations of the experiment.

5. Discussion and perspectives

GERDA is currently taking data, featuring an extremely low background at $Q_{\beta\beta}$ of 10^{-3} cts/(keV·kg·yr). The background is low enough to make the experiment background-free for the entire design exposure of 100 kg·yr and to make the sensitivity grow linearly with exposure. In spite of the much smaller exposure, the GERDA physics performance is comparable with the leading ^{136}Xe experiments, thanks to the superior background level and energy resolution. The

sensitivity on $T^{0\nu}_{1/2}$ reported here for ^{76}Ge ($5.8 \cdot 10^{25}$ yr), is slightly better than what is obtained by KamLAND-Zen for ^{136}Xe, $5.6 \cdot 10^{25}$ yr [9]. Taking the unblinded data into account, GERDA has currently the record sensitivity on $T^{0\nu}_{1/2}$. The Phase II background, normalized to the energy resolution and to the total efficiency (i.e. $B{\cdot}\mathrm{FWHM}/\epsilon$), is 5 (20) counts/(ton·yr) for BEGe (coaxial) detectors, namely a factor of five - or more - better than any competing non-^{76}Ge experiment.

GERDA is currently accumulating data. Taking into account the background level achieved so far and 11.2 kg·yr of still-to-be-unblinded coaxial data, the median sensitivity will break the wall of 10^{26} yr within 2018. The sensitivity expected for the full 100 kg·yr exposure of GERDA is about $1.4 \cdot 10^{26}$ yr. Furthermore, the excellent energy resolution makes GERDA very well suited for a possible discovery of $0\nu\beta\beta$ decay: with $\mathcal{E}$=100 kg·yr, a 3σ evidence of $0\nu\beta\beta$ decay could be claimed with 50%-chance for $T^{0\nu}_{1/2}$ up to $\sim 8 \cdot 10^{25}$ yr. A discussion of discovery potentials for present and future $0\nu\beta\beta$ experiments can be found in Ref. [26].

After the end of GERDA Phase II in 2019, the newly formed LEGEND Collaboration plans to operate up to 200 kg of $^{\mathrm{enr}}$Ge detectors in the existing GERDA infrastructure at Gran Sasso [27]. In order to maintain the background-free regime up to 1000 kg·yr exposure, a background reduction by a factor of 5-10 with respect to GERDA is aimed for. The second stage of LEGEND would be a 1-ton ^{76}Ge background-free experiment: such an ultimate experiment would reach a sensitivity of 10^{28} yr, and hence fully cover the inverted hierarchy region, in ten years of data taking.

References

[1] Schechter J and Valle J W F 1982 *Phys. Rev.* **D25** 2951
[2] Duerr M, Lindner M and Merle A 2011 *JHEP* **06** 091
[3] Davidson S, Nardi E and Nir Y 2008 *Phys. Rept.* **466** 105–177
[4] Mohapatra R N *et al.* 2007 *Rept. Prog. Phys.* **70** 1757–1867
[5] Päs H and Rodejohann W 2015 *New J. Phys.* **17** 115010
[6] Agostini M *et al.* (GERDA) 2017 *Nature* **544** 47
[7] Guiseppe V *et al.* (Majorana) 2017 The Status and Initial Results of the MAJORANA DEMONSTRATOR Experiment *MEDEX'17 meeting* (*Preprint* 1708.07562)
[8] Albert J *et al.* (EXO-200) 2014 *Nature* **510** 229–234
[9] Gando A *et al.* (KamLAND-Zen) 2016 *Phys. Rev. Lett.* **117** 082503
[10] Albert J *et al.* (EXO-200) 2017 (*Preprint* 1707.08707)
[11] Alfonso K *et al.* (CUORE) 2015 *Phys. Rev. Lett.* **115** 102502
[12] Andringa S *et al.* (SNO+) 2015 *Adv. High Energy Phys.* **2016** 6194250
[13] Ackermann K H *et al.* (GERDA) 2013 *Eur. Phys. J.* **C73** 2330
[14] Klapdor-Kleingrothaus H V *et al.* (Heidelberg-Moscow) 2001 *Eur. Phys. J.* **A12** 147–154
[15] Aalseth C E *et al.* (IGEX) 2002 *Phys. Rev.* **D65** 092007
[16] Budjáš D, Barnabé Heider M, Chkvorets O, Khanbekov N and Schönert S 2009 *JINST* **4** P10007
[17] Agostini M *et al.* (GERDA) 2013 *Eur. Phys. J.* **C73** 2583
[18] Agostini M, Pandola L, Zavarise P and Volynets O 2011 *JINST* **6** P08013
[19] Agostini M *et al.* (GERDA) 2013 *Phys. Rev. Lett.* **111** 122503
[20] Agostini M, Pandola L and Zavarise P 2012 *J. Phys. Conf. Ser.* **368** 012047
[21] Agostini M *et al.* (GERDA) 2015 *Eur. Phys. J.* **C75** 255
[22] Agostini M, Bellotti E, Brugnera R, Cattadori C M, D'Andragora A, di Vacri A, Garfagnini A, Laubenstein M, Pandola L and Ur C A 2011 *JINST* **6** P04005
[23] Victoria Wagner 2017 *Pulse Shape Analysis for the GERDA Experiment to Set a New Limit on the Half-life of $0\nu\beta\beta$ Decay of ^{76}Ge* Ph.D. thesis Univ. Heidelberg doi:10.11588/heidok.00022621
[24] Andrea Kirsch 2014 *Search for the Neutrinoless Double β-decay in* GERDA *Phase I Using a Pulse Shape Discrimination Technique* Ph.D. thesis Univ. Heidelberg doi:10.11588/heidok.00017149
[25] Cowan G, Cranmer K, Gross E and Vitells O 2011 *Eur. Phys. J.* **C71** 1554 [Erratum: Eur. Phys. J.C73,2501(2013)]
[26] Agostini M, Benato G and Detwiler J 2017 *Phys. Rev.* **D96** 053001
[27] Abgrall N *et al.* (LEGEND) 2017 The Large Enriched Germanium Experiment for Neutrinoless Double Beta Decay (LEGEND) *MEDEX'17 meeting* (*Preprint* 1709.01980)